

# Tourism Demand Forecasting with Tourist Attention: An Ensemble Deep Learning Approach

Shaolong Sun<sup>a</sup>, Yanzhao Li<sup>a</sup>, Shouyang Wang<sup>b,c,d</sup>, Ju-e Guo<sup>a,\*</sup>

<sup>a</sup>School of Management, Xi'an Jiaotong University, Xi'an 710049, China

<sup>b</sup>Academy of Mathematics and Systems Science, Chinese Academy of Sciences, Beijing 100190, China

<sup>c</sup>School of Economics and Management, University of Chinese Academy of Sciences, Beijing 100190, China

<sup>d</sup>Center for Forecasting Science, Chinese Academy of Sciences, Beijing 100190, China

\*Corresponding author. School of Management, Xi'an Jiaotong University, Xi'an 710049, China.

Tel: +86 130 9693 8376; Fax: +86 29 82665049.

E-mail address: [guojue@mail.xjtu.edu.cn](mailto:guojue@mail.xjtu.edu.cn) (J. E. Guo).

**Abstract:** The large amount of tourism-related data presents a series of challenges for tourism demand forecasting, including data deficiencies, multicollinearity and long calculation times. A bagging-based multivariate ensemble deep learning approach integrating stacked autoencoders and kernel-based extreme learning machines (B-SAKE) is proposed to address these challenges in this study. We forecast tourist arrivals in Beijing from four countries by adopting historical data on tourist arrivals in Beijing, economic indicators and online tourist behavior variables. The results from the cases of four origin countries suggest that our proposed B-SAKE approach outperforms than benchmark models in terms of horizontal accuracy, directional accuracy and statistical significance. Both bagging and stacked autoencoder can improve the forecasting performance of the models. Moreover, the forecasting performance of the models is evaluated with consistent results by means of the multi-step-ahead forecasting scheme.

**Keywords:** Tourism demand forecasting; Google trends; Stacked autoencoder; Bagging; Ensemble deep learning

## 1. Introduction

In recent years, with its rich tourism resources and strong cultural background, China has become an important tourist destination in the world, and the tourist volume in China has increased steadily. From 2015 to 2018, the tourist volume in China increased from 25.99 million to 30.54 million. Both the government and tourism practitioners need to implement corresponding measures based on the results of tourism demand forecasting. In addition, the perishability of tourism products makes tourism demand forecasting especially important (Chu, 2011; Shen, Li, & Song, 2008).

Current tourist demand forecasting techniques include various statistical, econometric, and artificial intelligence methods and combinations of these methods (Song & Li, 2008; Song, Qiu, & Park, 2019). Most of the early literature uses historical tourism demand data and certain economic variables to forecast future tourism demand. With the boom in Web search technology, a substantial number of web users seek information through search engines before taking a trip (Fesenmaier, Xiang, Pan, & Law, 2010). Therefore, search engine data could be used to accurately measure tourists' attention. Because search engine data are available and updated quickly, an increasing number of researchers have applied search engine data for forecasting different indicators, such as diseases (Ginsberg et al., 2009), consumer levels (Carrière-Swallow & Labbé, 2013) and tourism demand (Bangwayo-Skeete & Skeete, 2015). Beyond that, a set of effective methods for keyword selection and data aggregation to form the indicator has been gradually established (Li, Pan, Law, & Huang, 2017; Yang, Pan, Evans, & Lv, 2015). Obviously, search engine data, as a new type of predictor, can help further improve tourism demand forecasting accuracy. According to the concept of "data-intensive forecasting" proposed by Bunn (1989), a way to further improve forecast accuracy is by taking advantage of the availability of multiple information and computing resources. Song, Gao, and Lin (2013) point out that combining forecasts based on different methods or data has emerged as one of the most important ways to improve forecasting performance. Based on this modeling idea, this study incorporates search engine data, economic variables and the historical tourism demand data into the forecasting framework.

Nevertheless, introducing large amounts of data also poses huge challenges for forecasting. First, the large amount of data corresponds to many indicators potentially affecting tourism demand. As the number of potentially influential factors increases, the available training data in the feature space become increasingly sparse (Law, Li, Fong, & Han, 2019). Second, there is serious multicollinearity between independent variables, which affects the accuracy of forecasting (Li, Xu, Tang, Wang, & Li, 2018). Last and the most overlooked point in academic research, a model containing large

amounts of data means large increases in computations, which is impractical for application and promotion.

To address these challenges, a bagging-based multivariate ensemble deep learning model, integrating stacked autoencoders and kernel-based extreme learning machines (B-SAKE) is proposed for tourism demand forecasting. Deep learning techniques provide a mechanism of feature engineering that extracts discriminative features with minimal domain knowledge and human effort (Pouyanfar et al., 2018). Li, Chen, Wang, and Ming (2018) utilize principal component analysis (PCA) to compress the number of input variables and the redundant information in the input variables can be effectively reduced. Stacked autoencoder is capable of learning nonlinear relationships, which can be thought of as a more powerful nonlinear generalization of PCA. Bagging generates multiple data sets for training a set of base models to improve the stability of forecasting (Athanasopoulos, Song, & Sun, 2017; Inoue & Kilian, 2008). Kernel-based extreme learning machines have a short computing time and good generalization ability (Sun, Wei, Tsui, & Wang, 2019).

We conduct numerical experiments that use data related to travel demand, including historical data on tourist arrivals in Beijing, economic indicators and online tourist behavior variables. To further verify the effectiveness and robustness of the models, we consider four cases of forecasting tourist arrivals from four countries and multistep-ahead forecasting. The empirical study results reveal that our proposed B-SAKE model is the most accurate regarding the performance evaluation criteria, and that this model performs better than other benchmark models from a statistical perspective. In addition, the consistency of our findings across four countries we considered is encouraging.

The rest of this study is organized as follows. The Literature review section details the related literature on tourism demand forecasting with search engine data, and socioeconomic issue forecasting with deep learning. The Methodology section describes the conceptual framework of tourism demand forecasting with deep learning. The Empirical study section provides a case study on Beijing tourist arrivals and compares the results with those of benchmark models. Finally, conclusions and managerial implications are summarized in the Conclusions section.

## **2. Literature review**

### **2.1 Forecasting tourism demand with search engine data**

Search engine data, such as Google Trends, provide a time series index of the volume of queries users enter into a search engine in a given geographic area (Choi & Varian, 2012). In terms of tourism, travelers use search engines to find relevant

information regarding all aspects of a trip, including accommodations, attractions, activities, and dining (Fesenmaier et al., 2010). Therefore, a large amount of literature has incorporated search engine data into travel demand forecasts.

Choi and Varian (2012) first introduce Google Trends data to forecasting visitor arrivals in Hong Kong, and the positive effect of Google Trends data in forecasting is demonstrated by using visitor arrival data from nine source countries. However, they only consider the Google Trends index for “Vacation Destinations/Hong Kong”, and the way they aggregate the data results in information loss. Given these problems, Bangwayo-Skeete and Skeete (2015) propose a new indicator for tourism demand forecasting for countries in the Caribbean, which is based on a composite search for “hotels and flights”. They employ the mixed-data sampling (MIDAS) approach to fully utilize Google’s weekly data. The forecast results reveal that the AR-MIDAS model with the new indicator outperforms the SARIMA and AR models. Yang et al. (2015) point out that localized search engine data should be selected by comparing the fitness and forecasting power of Google Trends with Baidu Index. The systemic search query selection mechanism they proposed is widely accepted by later literature. Li, Wu, Peng, and Lv (2016) consider the noise contained in search engine data and tourism volumes and propose a model with denoising and forecasting by search engine data, namely CLSI-HHT (Hibert-Huang Transform), on the basis of CLSI (composite leading search index) proposed by Liu, Chen, Wu, Peng, and Lv (2015). The results demonstrate that the index model without denoising performs nearly the same as the time series model, while the CLSI-HHT model outperforms the baselines significantly. Li et al. (2017) focus on search engine data aggregation methods in the context of a large number of studies incorporating increasingly web search keywords. They adopt a generalized dynamic factor model (GDFM) to process many keyword variables and the findings suggest that the proposed method improves the forecast accuracy over those of two benchmark models: a traditional time series model and a model with an index created by principal component analysis (PCA). In recent years, some scholars have paid attention to spurious patterns in Google Trends data (see Bokelmann and Lessmann (2019), such as changes in search behavior and total search volume) and the language and platform biases that inevitably result from using search engine data (see Dergiades, Mavragani, and Pan (2018)), and they proposed corresponding improvement measures.

## **2.2 Forecasting socioeconomic issue with deep learning**

Artificial intelligence models have achieved successful applications in socioeconomic issue forecasting. However, the majority of the machine learning methods covered in the forecasting literature are shallow architectures, which have limited capabilities for exploring higher nonlinearities, particularly when the data have

large-scale and unclear patterns. In recent years, the application of deep learning methods has provided much potential for improving the forecasting performance for various socioeconomic issues.

Zhao, Li, and Yu (2017) propose a deep learning ensemble approach named SDAE-B (stacked denoising autoencoders-bagging) due to the complex relationship between crude oil price and various factors, and SDAE-B performs better than benchmark models including econometric models (i.e., RW and MRS), machine learning models with shallow architectures (i.e., SVR, SVR-B, FNN, and FNN-B) and its base model SDAE. Lv, Peng, and Wang (2018) propose an effective deep learning technique called the stacked autoencoder with echo-state regression (SAEN) to accurately forecast tourism demand based on search engine data. The results indicate that SAEN is better than the current methods, including time series approach, econometric model, common machine algorithms, and state-of-the-art deep learning techniques. Law et al. (2019) come up with two challenges (feature engineering and lag order selection) that traditional tourism demand forecasting models may face when massive amounts of search engine data are adopted as tourism demand indicators. And a deep network architecture for tourism demand forecasting based on LSTM augmented with the attention mechanism is proposed, which not only overcomes the two challenges mentioned above, but also significantly outperforms support vector regression (SVR) and artificial neural network (ANN) models. Considering the higher irregularity and volatility of individual loads in smart grids, Yang, Hong, and Li (2019) first combine deep ensemble learning with multitask representation learning and provide a new perspective for accurate probabilistic load forecasting for individual consumers. To fully exploit more hidden information in wind power historical data, Yin, Ou, Huang, and Meng (2019) apply a cascaded deep learning model to extract the implicit meteorological and temporal characteristics of each subseries generated by a two-layer mode decomposition method. Yang and Chen (2019) propose a wind speed forecasting model, namely E-S-ELM, which is hybridized by empirical mode decomposition (EMD), stacked autoencoders (SAE), and an extreme learning machine (ELM), where SAE develops a deep architecture for the forecasting model and ELM provides a fast learning speed and decent generalization capability. Aiming at the problem of multivariate time series forecasting problems, Sagheer and Kotb (2019) propose a pre-trained LSTM based stacked autoencoder (LSTM-SAE) approach in an unsupervised learning fashion instead of the random weight initialization strategy adopted in deep LSTM recurrent networks. Maqsood et al. (2020) acknowledge that stock markets are volatile and change abruptly due to the economic conditions, political situations and major events in a country. They take a dataset of a total of 11.42 million

tweets for eight mega-events from 2012-2016 and use them for efficient stock forecasting using deep learning.

### 3. Related methods

#### 3.1 Stacked autoencoder

A stacked autoencoder is a neural network consisting of multiple layers of autoencoders. An autoencoder, where the output is supposed to reconstruct the input, is a single hidden layer feedforward neural network. The structure of an autoencoder is shown in **Fig. 1**, in which  $X_I$ ,  $H$  and  $X_O$  are the input, output and hidden layer vectors, respectively;  $W_1$  is the weight matrix from the input layer to the hidden layer;  $W_2$  is the weight matrix from the hidden layer to the output layer; and  $b_1$  and  $b_2$  are the bias vectors of the input layer and the hidden layer, respectively. In an autoencoder, “encoding” refers to the transformation from  $X_I$  to  $H$ , and “decoding” refers to the transformation from  $H$  to  $X_O$ . The autoencoder tries to approximate an identity function to ensure that the input vector  $X_I$  is close to the output vector  $X_O$  and realizes the compressed and high-level representation of  $X_I$ , which is the hidden layer vector  $H$ . Consequently, an autoencoder is usually chosen to extract nonlinear features.

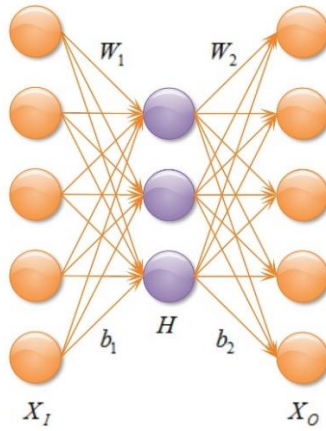


**Fig. 1** The structure of an autoencoder.

**Fig. 2** presents the structure of a stacked autoencoder, where the hidden layer output of the previous autoencoder is regarded as the input of the next autoencoder. Given complex sample data, SAE can hierarchically learn effective representations from the raw input and automatically filter irrelevant features. Directly training SAE across the entire structure is time-consuming and may result in the vanishing gradient problem, particularly if the network depth is large. Layer-wise training has been the core of deep neural network (DNN) learning. In the case of SAE, each autoencoder in SAE is first trained by the back propagation (BP) algorithm in a sequential and

unsupervised manner. Thereafter, the updated parameters of SAE are shared and maintained. After layer-wise training, the SAE parameters can obtain their local optimum values.

As a deep representation learning approach, SAE is insensitive to the raw input features. Accordingly, this robustness reduces the necessity of artificial feature prescreening.

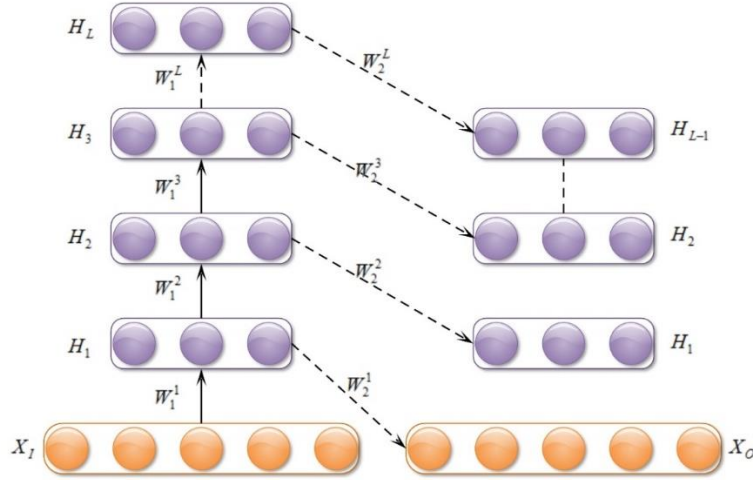


**Fig. 2** Stacked autoencoder structure.

### 3.2 Kernel extreme learning machine

Extreme learning machine (ELM), which was proposed by Huang, Zhu, and Siew (2006), is a type of single-hidden layer feedforward neural network (SLFN). The ELM model has been widely applied to many fields due to its fast learning speed and generalization ability. The key highlight of the ELM model is that the input weights and biases are randomly generated and the hidden layer parameters do not need to be adjusted. The output weights are obtained by simple matrix computations, so the computing time is very short.

For  $N$  arbitrary samples  $(x_i, y_i)$ ,  $x_i \in \mathfrak{R}^N$ ,  $y_i \in \mathfrak{R}^N$ , and  $i = 1, 2, \dots, N$ . If the activation function of the hidden layer is  $h(x)$  and the output matrix is  $Y$ , then the typical SLFNs can be defined as

$$Y = \begin{bmatrix} y_{1j} \\ y_{2j} \\ \vdots \\ y_{mj} \end{bmatrix}_{m \times N} = \begin{bmatrix} \sum_{i=1}^l \beta_{i1} h(\omega_i x_j + b_i) \\ \sum_{i=1}^l \beta_{i2} h(\omega_i x_j + b_i) \\ \vdots \\ \sum_{i=1}^l \beta_{im} h(\omega_i x_j + b_i) \end{bmatrix}_{m \times N} \quad j = 1, 2, \dots, N \quad (1)$$

where  $\beta$  represents the network output weights between the hidden layer and the output layer,  $\omega_{ij}$  is the input weight between the input layers and the hidden layers,  $l$  is the number of hidden nodes and  $b$  is the threshold of the hidden layer. The above equations can also be written as:

$$H\beta = Y, \quad Y \in \mathbb{R}^{N \times m}, \beta \in \mathbb{R}^{N \times m}, \quad H = H(\omega, b) = h(\omega x + b) \quad (2)$$

where  $H$  is the output matrix of the hidden layer. The input weights and biases are randomly produced instead of being tuned according to Huang. The only unknown parameter is the output weight  $\beta$  which can be solved by the ordinary least squares (OLS) method. The solution of the above equation is given by

$$\hat{\beta} = H^\dagger Y, \quad H^\dagger = H^T (HH^T)^{-1} \quad (3)$$

where  $H^\dagger$  represents the Moore-Penrose generalized inverse of a matrix  $H$ . According to Ridge regression theory and the orthogonal projection method,  $\beta$  can be calculated by adding a positive penalty factor  $1/C$  as follows:

$$\hat{\beta} = H^T (1/C + HH^T)^{-1} Y \quad (4)$$

Then, the output function of the ELM can be expressed as

$$f(x) = H \hat{\beta} = HH^T (1/C + HH^T)^{-1} Y \quad (5)$$

This method overcomes some shortcomings of the typical gradient-based learning algorithms, such as overfitting, local minima and long computation times. The topological structure of ELM is shown in **Fig. 3**.

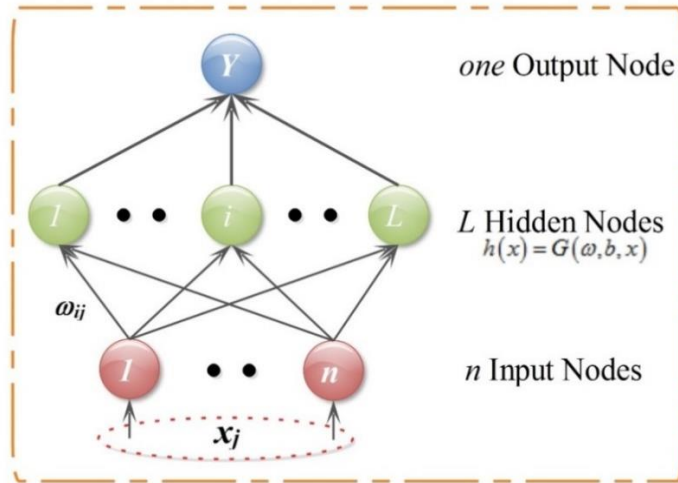


**Fig. 3** The topological structure of ELM.

A Kernel-based ELM was proposed by Huang (2014). The activation function  $h(x)$  of the hidden layer is replaced by a kernel function in terms of Mercer's conditions. The output function of the KELM can be formulated as:



$$f(x) = h(x) \hat{\beta} = \begin{bmatrix} k(x, x_1) \\ k(x, x_2) \\ \vdots \\ k(x, x_n) \end{bmatrix}^T (1/C + HH^T)^{-1} Y \quad (6)$$

In this formula, the feature mapping  $h(x)$  does not need to be known to users, instead one may use its corresponding kernel  $k(x, x_i)$ . This means that a kernel function can replace the random mapping of the ELM and make the output weights more stable. Therefore, the KELM achieves better generalization ability than the ELM. The Gaussian kernel function is employed in this study. In term of SAE procedure introduced in **Section 3.1**, the flowchart of our proposed SAE-based KELM (SAKE) tourism demand forecasting approach is shown in **Fig 4**.

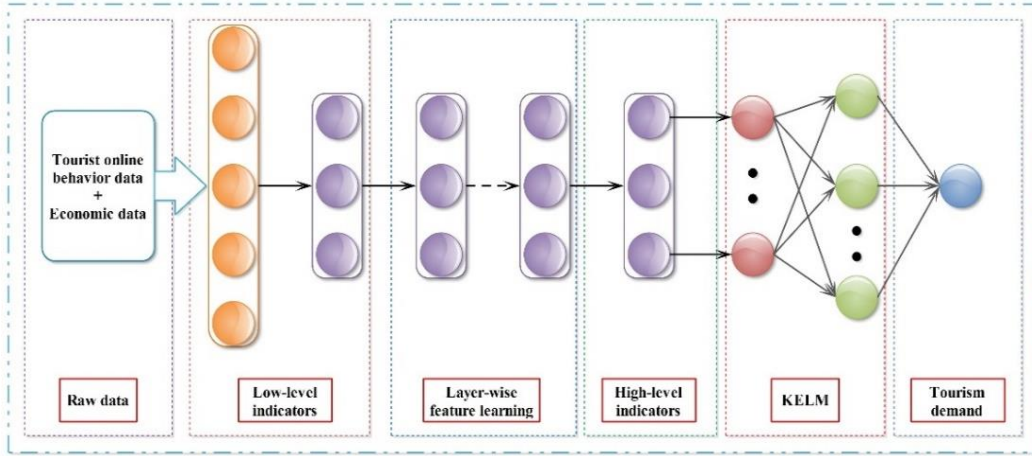


**Fig. 4** The flowchart of SAKE tourism demand forecasting approach.

### 3.3 Bagging

Bagging was originally introduced by Breiman (1996) to improve unstable procedures by generating new learning sets. In the forecasting context, the purpose of bagging is to reduce the variance in our forecast. Specifically, using the resampling technique, bagging generates additional samples for training our model by extracting and replacing data from the original data set. These additional samples are called “resampling samples”. We suppose that  $K$  samples are generated. For each sample, the procedure described in the above subsection for building the SAKE network is repeated for each resampling sample and forecasts are generated with each iteration. Therefore, we now have  $K$  sets of forecasts instead of one set of forecasts. To obtain the final forecast, we aggregate over these  $K$  forecasts by taking the average or the median, which results in a lower forecast variance than when using only one forecast from the original sample.

Bagging forecasting involves generating a larger number of samples, which are called bootstrap samples. Let  $y_t$  be a vector containing all the predictors at time  $t$  such that  $y_t = (1, l_t')$ . Suppose that the total number of in-sample data points is  $T$ , hence  $X_T$  represents the most latest observation. The in-sample data are arranged through a matrix of dimensions  $(T-h) \times (1+q)$  shown as follows:

$$B = \begin{bmatrix} x_{1+h} & y_1' \\ \vdots & \vdots \\ x_T & y_{T-h}' \end{bmatrix} \quad (7)$$

We generate a bootstrap sample  $k$  by drawing a replacement from the matrix  $B$  blocks of  $m$  rows so that the dependence in the error term is captured. This can be expressed as follows:

$$B^{(k)} = \begin{bmatrix} x_{1+h}^{(k)} & y_1'^{(k)} \\ \vdots & \vdots \\ x_T^{(k)} & y_{T-h}'^{(k)} \end{bmatrix} \quad (8)$$

For each bootstrap sample, we implement model selection and estimate the model from matrix  $B^{(k)}$  blocks. We fit the model back to the most recent observations in the matrix  $B$  blocks and obtain forecast  $\hat{x}_{T+h}^{(k)}$ . We repeat the process for  $k = 1, 2, \dots, K$ . Then the final forecast is obtained as follows:

$$\hat{x}_{T+h}^{(bag)} = \frac{1}{K} \sum_{k=1}^K \hat{x}_{T+h}^{(k)} \quad (9)$$

In this study, the bootstrap samples  $K = 100$  are based on Inoue and Kilian (2008). For more details about bagging, please refer to Breiman (1996).

### 3.4 Multivariate forecasting

Multivariate forecasting, unlike univariate forecasting, considers not only the autoregressive effect of the target series but also the effect of the exogenous variable on the target series. This can be denoted by

$$y(t+m) = f(s(y), s(x_1), \dots, s(x_c)) \quad (10)$$

where  $y(t+m)$  is the value of the dependent variable at time  $t+m$ , and  $s(x) = x(t), x(t-1), \dots, x(t-N_x+1)$  is a set of past values of exogenous variable  $x$  with a total number of  $N_x$ . Thus the input size is  $S = \sum N_y + N_{x_1} + N_{x_2} + \dots + N_{x_c}$ .

### 3.5 Ensemble deep learning approach

**Fig. 5** shows the flowchart of the overall process of our proposed ensemble deep

learning approach. The B-SAKE ensemble learning approach proposed in this study is generally composed of the following five main steps:

**Data preprocessing:** transform and partition the multidimensional data into in-sample datasets and out-of-sample datasets.

**Bootstrapping processing:** generate  $K$  sets of replicas of the in-sample datasets by the bagging method.

**Model training processing:** train  $K$  SAKE models with each set of the in-sample datasets independently.

**Individual forecasting processing:** generate  $W$  forecasts though using the  $K$  trained SAKE models.

**Ensemble learning processing:** take the mean value of the  $W$  forecasts as the final forecasting results.

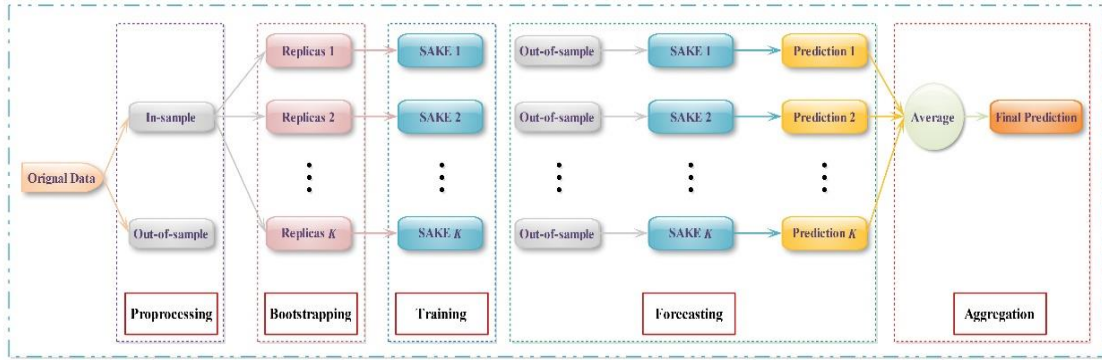


**Fig. 5** The process of the B-SAKE ensemble deep learning approach.

## 4. Empirical study

In this section, the forecasting performance of our proposed B-SAKE is tested against benchmark models. First, the dataset description is introduced in **Section 4.1**. Second, the forecasting performance evaluation criteria and statistical tests are given in **Section 4.2**. Third, the benchmarks and parameter settings are introduced in **Section 4.3**. Finally, the results and relevant analysis are given in **Section 4.4**.

### 4.1 Dataset

#### 4.1.1 Dependent variable

In this study, tourist demand (described by tourist arrivals) is investigated for forecasting purposes. We select monthly inbound tourist arrivals in Beijing city over the period January 2008 to December 2018 from origin countries of Germany, France, the United Kingdom, and the United States, which is shown in **Fig. 6**. It is clearly observed that tourist arrivals show seasonality and volatility. The United States is the largest source of tourists for Beijing city within the four countries. The historical

datasets are collected from the Wind Database (<https://www.wind.com.cn/>). The datasets are divided into the in-sample subset and the out-of-sample subset. The in-sample subset is used for model training with data from 2008.1 to 2016.12, while the out-of-sample subset is used for model testing with data from 2017.1 to 2018.12.

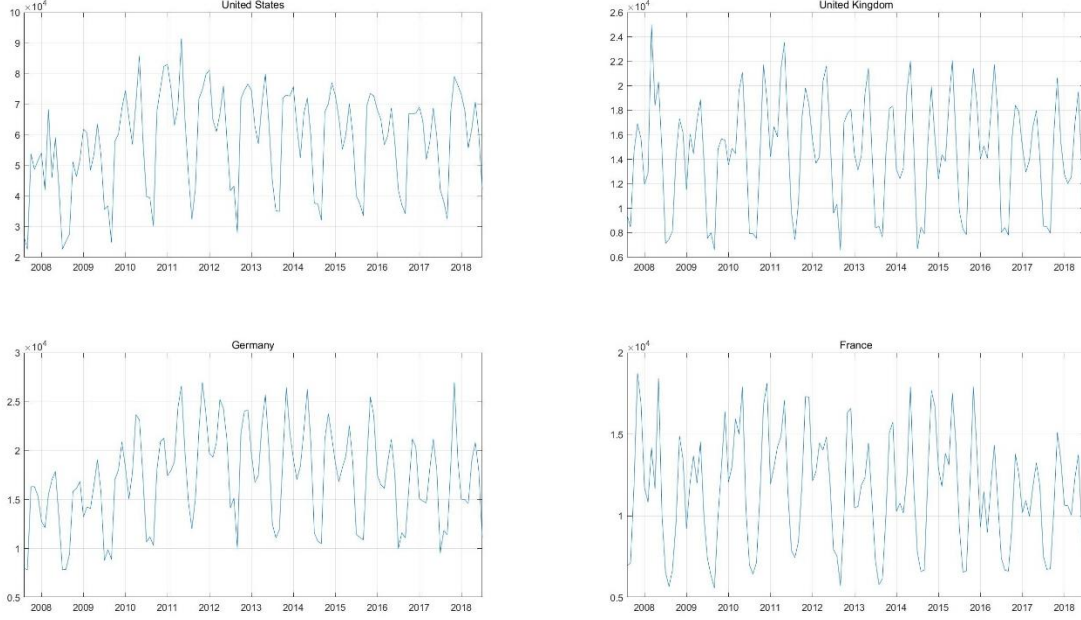


**Fig. 6** Tourist arrivals in Beijing city from four countries.

#### 4.1.2 Economic variables

The demand for a service or good is inversely related to its price, which is stated by the law of demand. This is measured by the price variable, defined as the ratio between CPIs and standardized by exchange rate:

$$P_{i,t} = \frac{CPI_{CN,t} / EX_{i,t}^{CNY}}{CPI_{i,t}} \quad (11)$$

where  $i = 1, 2, \dots, n$  represents the  $n$  source countries,  $CPI_{i,t}$  represents the CPI of the source country  $i$  at time  $t$ , and  $EX_{i,t}^{CNY}$  is the exchange rate between China Yuan and the currency of the origin country  $i$ .

Furthermore, the demand for a service or good is also affected by the prices of substitute and/or complementary goods. For travel destinations, South Korea and Japan seem to be alternative options to China, and the substitute prices are defined as

$$S_{i,t}^{KR} = \frac{CPI_{KR,t}}{EX_{i,t}^{KRW}} \text{ and } S_{i,t}^{JP} = \frac{CPI_{JP,t}}{EX_{i,t}^{JPY}} \quad (12)$$

It is expected that tourists' income positively influences tourism demand, which is often measured by the gross domestic product (GDP).

$$GDP_{i,t} \quad (13)$$

The final economic variable we considered is the interest rate spread defined as

$$IRS_{i,t} = LTGB_{i,t} - STGB_{i,t} \quad (14)$$

where  $LTGB_{i,t}$  is the long-term 10-year government bond and  $STGB_{i,t}$  is the short-term 90-day government bill of the source country. This variable has been widely used in the economic literature (see Stock and Watson (2012); Anderson, Athanasopoulos, and Vahid (2007); Athanasopoulos, Hyndman, Song, and Wu (2011)). Datasets of the economic variables mentioned above are also collected from the Wind Database (<https://www.wind.com.cn/>).

#### 4.1.3 Tourist online behavior variables

We follow X. Yang et al. (2015) and choose 24 basic search keywords in Google Trend based on the destination and various dimensions of tourism planning, including tour, lodging, recreation, traffic, dining, and shopping. The basic search keywords related to Beijing tourism are listed in **Table 1** with their corresponding dimensions. Then we search for the basic keywords in a specific country of origin and set iteratively recommended keywords as the next round of search keywords. This process is repeated until there are no new keywords in the recommended list. Finally, we obtain 51 keywords, 45 keywords, 38 keywords and 33 keywords for the United States, the United Kingdom, Germany and France, respectively.

**Table 1** Basic search keywords related to Beijing tourism.

Dimension	Keywords	Dimension	Keywords	Dimension	Keywords
Tour	Beijing travel	Lodging	Beijing hotels	Recreation	Beijing recreation
	Beijing travel agency		Beijing accommodation		Beijing night life
	Beijing weather		Beijing restaurant		Beijing bar
	Beijing maps		Beijing resorts		Beijing show
Traffic	Beijing airlines	Dining	Peking duck	Shopping	Beijing shopping
	Beijing flights		Beijing food		Beijing shopping guide
	Beijing airports		Beijing food guide		Dashilan Street
	Beijing subway		Beijing snack		Panjiayuan Center

We calculate the Pearson correlation coefficient between inbound tourist arrivals and each of the keywords with different lag periods. Four correlation coefficients are calculated for each search keyword, including the correlations between the visitor volumes in the current period and search query volumes from 1-4 months prior. We

choose the keywords with the highest correlation coefficient values, which are shown in **Table 2**. To obtain the appropriate numbers of keywords, we use 0.7 as the threshold for the correlation coefficient, in other words, we select the keywords with a correlation coefficient value greater than 0.7. It can be observed that the optimal lag order of most keywords is 1, indicating that tourists retrieve travel-related information one month in advance.

**Table 2** Maximum correlation coefficient of search keywords.

Countries	Keywords	Lag order	Countries	Keywords	Lag order
US	Beijing travel	3	UK	China travel	2
	Beijing weather	2		Beijing travel	2
	China travel	2		Beijing travel agency	2
	Beijing airlines	1		Beijing airlines	1
	Beijing flights	1		Beijing flights	1
	Beijing airports	1		Beijing airports	1
	Beijing subway	1		Beijing hotels	1
	Beijing hotels	1		Beijing restaurant	1
	Beijing restaurant	1		Peking duck	1
	Peking duck	1		Duck recipes	1
	Duck recipes	1		Beijing shopping	1
	Beijing shopping	1		Great Wall	1
	Great Wall	1		Beijing maps	1
	Forbidden city	1			
Germany	Beijing travel	3	France	Beijing tourism	3
	Beijing maps	2		Beijing travel	2
	Beijing weather	2		Beijing weather	2
	China travel	2		Beijing flights	1
	Peking duck	1		Beijing airports	1
	Beijing shopping	1		Beijing hotels	1
	Great Wall	1		Beijing shopping	1
	Beijing airlines	1		Peking duck	1
	Beijing flights	1		Great Wall	1
	Beijing airports	1		Forbidden city	1
	Beijing hotels	1			
	Beijing restaurant	1			

## 4.2 Performance evaluation criteria and statistical test

To evaluate the forecasting performance of models from level forecasting, two indicators, mean absolute percentage error (MAPE) and normalized root mean square error (NRMSE), have been frequently utilized in recent years.

$$MAPE = \frac{1}{N} \sum_{t=1}^N \left| \frac{x_t - \hat{x}_t}{x_t} \right| \quad (15)$$

$$NRMSE = \frac{1}{\bar{x}} \sqrt{\frac{1}{N} \sum_{t=1}^N (x_t - \hat{x}_t)^2} \quad (16)$$

The performance in forecasting the direction of movement can be measured by a directional symmetry (DS) as follows:

$$DS = \frac{1}{T} \sum_{t=2}^T d_t \times 100\%, \text{ where } d_t = \begin{cases} 1 & \text{if } (x_t - x_{t-1})(\hat{x}_t - x_{t-1}) > 0 \\ 0 & \text{otherwise} \end{cases} \quad (17)$$

where  $N$  is the number of observations in the datasets,  $x_t$  and  $\hat{x}_t$  represent the true value and the forecasting value at time  $t$ , respectively. MAPE and NRMSE measure the level accuracy, the smaller the MAPE and NRMSE are, the better the level performance. DS measures the directional accuracy, the higher the DS is, the better the directional performance.

To further compare the horizontal forecasting accuracy of different forecasting models from the statistical perspective, we use the DM test to test the statistical significance of different forecasting models (Diebold & Mariano, 2002). The DM test is mainly used to test the null hypothesis that the forecasting ability of different models is equal to the expected forecasting accuracy. We choose MSE as the loss function, and the null hypothesis is that the MAPE of test model A is not less than that of benchmark model B. The DM statistics are defined as follows:

$$S_{DM} = \frac{\bar{g}}{\sqrt{\hat{V}_{\bar{g}}/T}} \quad (18)$$

where  $\bar{g} = \sum_{t=1}^T g_t / T$ ,  $g_t = (x_t - \hat{x}_{A,t})^2 - (x_t - \hat{x}_{B,t})^2$ ,  $\hat{V}_{\bar{g}} = \gamma_0 + 2 \sum_{l=1}^{\infty} \gamma_l$  and  $\gamma_l = \text{cov}(g_t, g_{t-l})$ . We note that  $\hat{x}_{A,t}$  and  $\hat{x}_{B,t}$  represent the forecasting value of the test model A and the benchmark model B at time  $t$ , respectively. In the DM test, the null hypothesis is rejected when  $S_{DM}$  and the p-value are less than the significance level, otherwise, the null hypothesis cannot be rejected.

In addition, we use the PT test to compare the directional forecasting accuracy of different forecasting models (Pesaran & Timmermann, 1992). In the PT test, the null hypothesis assumes that the true and forecast motion trends are independent of each other. Therefore, the PT statistics are asymptotically subject to a 0-1 distribution under the null hypothesis, which is defined as follows:

$$S_{PT} = \left[ \frac{P_*(1-P_*)}{T} \right]^{-\frac{1}{2}} (\hat{P} - P_*) \quad (19)$$

where  $\hat{P}$  is the proportional term that is correctly forecast based on the trend movement,  $\hat{P} = \frac{1}{T} \sum_{t=1}^T H_t [(\hat{x}_{t+1} - \hat{x}_t)]$ .  $P_*$  is the independent success rates of the

actual and forecast movement trend.  $p_1 = \frac{1}{T} \sum_{t=1}^T H_t[(x_{t+1} - x_t)]$ , where  $H(z)$  is the Heaviside function. Similarly, comparing  $S_{pT}$  with the corresponding  $p$  value, the directional forecasting ability of different models can be evaluated from the statistical perspective.

### 4.3 Benchmarks and parameter settings

To evaluate the forecasting performance of the B-SAKE models by means of the multistep-ahead forecasting scheme, we compare this approach with some other benchmark models. SARIMA is the most popular econometric model due to the seasonal periodicity of tourism demand data. The MLP and KELM models, as the most popular AI techniques, are widely used in tourism demand forecasting. We add stacked autoencoder network for dimension reduction on the basis of KELM to construct the SAKE model. In addition, we consider bagging-based (B-based) AI models, such as B-MLP, B-KELM, and B-SAKE.

The parameter specification is crucial for model performance. The parameters involved in this study are set based on previous literature and adjusted by trial and error testing.

### 4.4 Empirical results

#### 4.4.1 Forecast evaluations

We evaluate the forecasting performance of our proposed B-SAKE model and the six benchmark models mentioned above employing the MAPE, NRMSE, and DS evaluation criteria. To further test the effectiveness of the forecasting models, multistep-ahead forecasting scheme is adopted. We consider 1-month-ahead forecasting, 3-month-ahead forecasting, and 6-month-ahead forecasting. The results are displayed in **Tables 3-5**.

From **Tables 3-5**, it can be summarized that: (1) B-SAKE is the most accurate approach compared with the benchmark models in terms of the MAPE, NRMSE, and DS criteria. (2) The B-based models generally outperform than the original models in forecasting accuracy. (3) As we expected, SAKE, an SA neural network added to KELM for dimension reduction, has better forecasting performance than KELM. (4) The SARIMA model is the worst benchmark model, possibly because SARIMA is not capable of efficiently capturing nonlinear patterns of tourism data in contrast to the AI models. (5) With the advance of forecasting time, the forecasting accuracy of all the models decreases.

In particular, our proposed B-SAKE model achieves the best forecasting accuracy in the four origin countries, which is shown in bold in the tables. Taking the example



of the United States, the reductions in MAPE are 90.89%, 87.41%, 76.70%, 75.58%, 68.92% and 34.96% in comparison with those of SARIMA, MLP, B-MLP, KELM, B-KELM and SAKE in the case of 1-month-ahead forecasting. For NRMSE the reductions are 89.80%, 85.60%, 79.31%, 78.64%, 69.86% and 33.33%, respectively. B-SAKE achieves 77.36% better directional forecasts than SARIMA and 20%-30% better directional forecasts than the AI models. It is clearly illustrated that our proposed B-SAKE model is a highly promising forecasting approach.

**Table 3** Forecasting performance of different models: 1-month-ahead forecasting.

Countries	Models	In-sample			Out-of-sample		
		MAPE	NRMSE	DS	MAPE	NRMSE	DS
US	SARIMA	5.413	6.019	55.21	5.935	6.843	54.17
	MLP	3.915	4.263	72.92	4.017	4.586	62.50
	B-MLP	2.116	2.968	78.13	2.873	3.514	66.67
	KELM	2.019	2.875	77.08	2.637	3.142	70.83
	B-KELM	1.586	2.037	79.17	1.781	2.364	75.00
	SAKE	0.758	0.921	86.46	0.895	1.002	83.33
	B-SAKE	<b>0.493</b>	<b>0.614</b>	<b>97.92</b>	<b>0.539</b>	<b>0.684</b>	<b>100.00</b>
UK	SARIMA	5.321	5.873	57.29	5.765	6.521	58.33
	MLP	3.874	4.301	73.96	4.115	4.453	66.67
	B-MLP	2.106	2.829	77.08	2.704	3.437	70.83
	KELM	2.113	2.807	76.04	2.638	3.012	75.00
	B-KELM	1.602	2.115	78.13	1.876	2.364	79.17
	SAKE	0.927	1.206	87.50	1.049	1.258	87.50
	B-SAKE	<b>0.583</b>	<b>0.705</b>	<b>95.83</b>	<b>0.639</b>	<b>0.794</b>	<b>95.83</b>
Germany	SARIMA	5.217	5.638	56.25	5.601	6.332	54.17
	MLP	3.746	4.105	75.00	4.015	4.307	66.67
	B-MLP	2.019	2.736	79.17	2.507	3.275	75.00
	KELM	2.005	2.693	78.13	2.439	2.982	75.00
	B-KELM	1.403	2.012	80.21	1.631	2.204	79.17
	SAKE	0.809	0.994	88.54	0.947	1.143	87.50
	B-SAKE	<b>0.514</b>	<b>0.621</b>	<b>100.00</b>	<b>0.548</b>	<b>0.683</b>	<b>95.83</b>
France	SARIMA	5.447	5.906	54.17	5.907	6.492	54.17
	MLP	3.896	4.251	71.88	4.206	4.517	62.50
	B-MLP	2.258	2.906	76.04	2.844	3.352	66.67
	KELM	2.165	2.884	76.04	2.608	3.108	70.83
	B-KELM	1.652	2.067	78.13	1.835	2.216	75.00
	SAKE	0.944	1.305	85.42	1.106	1.295	79.17
	B-SAKE	<b>0.613</b>	<b>0.745</b>	<b>93.75</b>	<b>0.701</b>	<b>0.785</b>	<b>91.67</b>

**Table 4** Forecasting performance of different models: 3-month-ahead forecasting.

Countries	Models	In-sample			Out-of-sample		
		MAPE	NRMSE	DS	MAPE	NRMSE	DS

		MAPE	NRMSE	DS	MAPE	NRMSE	DS
US	SARIMA	5.501	5.943	53.19	5.942	6.886	54.17
	MLP	3.896	4.128	57.45	4.109	4.593	58.33
	B-MLP	2.207	3.146	60.64	2.894	3.571	62.50
	KELM	2.158	3.053	65.96	2.729	3.203	62.50
	B-KELM	1.703	2.214	70.21	1.834	2.385	66.67
	SAKE	0.895	1.102	79.79	0.912	1.175	79.17
	B-SAKE	<b>0.584</b>	<b>0.739</b>	<b>90.43</b>	<b>0.613</b>	<b>0.794</b>	<b>87.50</b>
UK	SARIMA	5.408	5.886	55.32	5.802	6.613	54.17
	MLP	3.940	4.395	60.64	4.124	4.485	62.50
	B-MLP	2.251	3.058	68.09	2.718	3.445	66.67
	KELM	2.236	2.984	69.15	2.695	3.101	66.67
	B-KELM	1.742	2.205	73.40	1.925	2.397	70.83
	SAKE	1.025	1.374	82.98	1.139	1.402	79.17
	B-SAKE	<b>0.675</b>	<b>0.793</b>	<b>91.49</b>	<b>0.725</b>	<b>0.884</b>	<b>87.50</b>
Germany	SARIMA	5.321	5.759	52.13	5.711	6.425	45.83
	MLP	3.853	4.256	59.57	4.096	4.396	58.33
	B-MLP	2.127	2.858	63.83	2.617	3.364	62.50
	KELM	2.207	2.801	68.09	2.545	3.022	66.67
	B-KELM	1.526	2.106	72.34	1.726	2.307	70.83
	SAKE	0.915	1.145	78.72	1.021	1.253	75.00
	B-SAKE	<b>0.608</b>	<b>0.733</b>	<b>89.36</b>	<b>0.657</b>	<b>0.760</b>	<b>83.33</b>
France	SARIMA	5.514	6.004	51.06	6.014	6.583	50.00
	MLP	3.926	4.296	58.51	4.310	4.594	54.17
	B-MLP	2.338	2.988	64.89	2.896	3.412	58.33
	KELM	2.253	2.903	67.02	2.711	3.213	62.50
	B-KELM	1.751	2.175	71.28	1.905	2.305	70.83
	SAKE	1.031	1.412	77.66	1.217	1.309	75.00
	B-SAKE	<b>0.709</b>	<b>0.816</b>	<b>88.30</b>	<b>0.819</b>	<b>0.901</b>	<b>83.33</b>

**Table 5** Forecasting performance of different models: 6-month-ahead forecasting.

Countries	Models	In-sample			Out-of-sample		
		MAPE	NRMSE	DS	MAPE	NRMSE	DS
US	SARIMA	6.204	6.913	51.65	6.585	6.963	50.00
	MLP	5.873	5.943	56.04	6.036	6.147	54.17
	B-MLP	4.161	4.207	59.34	4.543	4.601	58.33
	KELM	4.035	4.352	63.74	4.167	4.375	62.50
	B-KELM	3.256	3.106	69.23	3.402	3.321	66.67
	SAKE	1.758	1.701	78.02	1.808	1.905	75.00
	B-SAKE	<b>1.142</b>	<b>1.235</b>	<b>87.91</b>	<b>1.236</b>	<b>1.343</b>	<b>83.33</b>
UK	SARIMA	6.385	6.749	52.75	6.601	6.835	54.17
	MLP	5.741	5.810	58.24	5.904	6.024	58.33
	B-MLP	4.359	4.361	62.64	4.498	4.535	62.50
	KELM	4.336	4.458	67.03	4.441	4.601	62.50

	B-KELM	3.104	3.267	72.53	3.517	3.358	66.67
	SAKE	1.837	1.901	81.32	1.934	2.043	79.17
	B-SAKE	<b>1.206</b>	<b>1.348</b>	<b>89.01</b>	<b>1.319</b>	<b>1.455</b>	<b>83.33</b>
Germany	SARIMA	6.103	6.258	50.55	6.214	6.359	45.83
	MLP	5.507	5.654	57.14	5.639	5.832	54.17
	B-MLP	4.124	4.235	60.44	4.147	4.353	58.33
	KELM	4.048	4.209	64.84	4.265	4.298	62.50
	B-KELM	2.943	3.036	70.33	3.107	3.104	66.67
	SAKE	1.714	1.854	76.92	1.851	1.985	70.83
	B-SAKE	<b>1.025</b>	<b>1.146</b>	<b>86.81</b>	<b>1.138</b>	<b>1.268</b>	<b>79.17</b>
France	SARIMA	6.269	6.437	51.65	6.585	6.731	45.83
	MLP	5.543	5.610	56.04	5.836	5.836	50.00
	B-MLP	4.301	4.411	61.54	4.501	4.602	54.17
	KELM	4.258	4.374	63.74	4.394	4.589	58.33
	B-KELM	3.043	3.165	69.23	3.452	3.293	58.33
	SAKE	1.804	1.987	75.82	1.991	2.120	70.83
	B-SAKE	<b>1.267</b>	<b>1.359</b>	<b>85.71</b>	<b>1.368</b>	<b>1.487</b>	<b>79.17</b>

#### 4.4.2 Statistical tests

To further verify the level and directional forecasting performance of the B-SAKE model from the statistical perspective, the DM test and the PT test are also employed to test the statistical significance of all the models within the out-of-sample. **Tables 6-9** demonstrate the results of the DM test and the PT test with respect to different forecasting horizons. The numbers outside the brackets in the table are the statistics while the numbers inside the brackets are the corresponding p-values.

According to the DM test results, we can observe that as the number of advance steps increases, the forecasting performance of the model decreases. Even so, when the B-SAKE model is tested, all the DM tests are less than -1.7013 corresponding to p-values less than 0.444, which means that the B-SAKE model outperforms other benchmark models under a 95% confidence level. This indicates the high performance of the B-SAKE model. In particular, we note that when the B-SAKE is tested against the SARIMA model, B-SAKE model statistically confirms its superiority at the 100% confidence level. Furthermore, Tables 6-8 show that the level forecasting performance of the models increases successively for SARIMA, MLP, B-MLP, KELM, B-KELM, SAKE and B-SAKE utilizing a multistep-ahead forecasting scheme.

The PT test results are reported in **Table 9**. The forecasting results of the B-SAKE model reject the null hypothesis near the 100% confidence level, which further reveals its powerful function and effectiveness.

**Table 6** The DM test results for different models in 1-month-ahead forecasting.

Countries	Models	B-SAKE	SAKE	B-KELM	KELM	B-MLP	MLP
-----------	--------	--------	------	--------	------	-------	-----

US	SAKE	-1.9873 (0.0234)						
	B-KELM	-2.0358 (0.0209)	-1.9461 (0.0258)					
	KELM	-2.3879 (0.0085)	-2.0133 (0.0220)	-1.8742 (0.0305)				
	B-MLP	-2.9367 (0.0017)	-2.5381 (0.0056)	-1.8943 (0.0340)	-1.8627 (0.0291)			
	MLP	-3.8749 (0.0001)	-3.4106 (0.0003)	-2.2033 (0.0014)	-2.1782 (0.0147)	-1.8658 (0.0310)		
	SARIMA	-4.5037 (0.0000)	-4.2917 (0.0000)	-4.0143 (0.0000)	-3.9741 (0.0000)	-3.2859 (0.0005)	-2.9576 (0.0016)	
UK	SAKE	-1.9560 (0.0252)						
	B-KELM	-1.9983 (0.0228)	-1.9562 (0.0252)					
	KELM	-2.2749 (0.0115)	-2.1247 (0.0168)	-1.8868 (0.0296)				
	B-MLP	-2.8907 (0.0019)	-2.4359 (0.0074)	-1.8856 (0.0297)	-1.8963 (0.0290)			
	MLP	-3.6358 (0.0001)	-3.4267 (0.0003)	-2.3748 (0.0088)	-2.2041 (0.0138)	-1.8742 (0.0305)		
	SARIMA	-4.4937 (0.0000)	-4.2341 (0.0000)	-4.1045 (0.0000)	-3.9648 (0.0000)	-3.3058 (0.0005)	-2.8937 (0.0019)	
Germany	SAKE	-1.9843 (0.0236)						
	B-KELM	-2.0687 (0.0193)	-1.9687 (0.0245)					
	KELM	-2.2975 (0.0108)	-2.1589 (0.0154)	-1.8963 (0.0290)				
	B-MLP	-2.9954 (0.0014)	-2.3946 (0.0083)	-1.8756 (0.0304)	-1.9354 (0.0265)			
	MLP	-3.7025 (0.0001)	-3.5085 (0.0002)	-2.4019 (0.0082)	-2.2241 (0.0131)	-1.8965 (0.0289)		
	SARIMA	-4.5136 (0.0000)	-4.3541 (0.0000)	-4.0157 (0.0000)	-4.0156 (0.0000)	-3.4523 (0.0003)	-2.9632 (0.0015)	
France	SAKE	-1.8994 (0.0288)						
	B-KELM	-1.9536 (0.0254)	-1.8713 (0.0307)					
	KELM	-2.1254 (0.0168)	-2.0145 (0.0220)	-1.8623 (0.0313)				
	B-MLP	-2.7412 (0.0031)	-2.3657 (0.0090)	-1.7843 (0.0372)	-1.9602 (0.0250)			
	MLP	-3.5896 (0.0002)	-3.3215 (0.0004)	-2.2250 (0.0130)	-2.2247 (0.0131)	-1.8690 (0.0308)		
	SARIMA	-4.3582 (0.0000)	-4.1598 (0.0000)	-4.0236 (0.0000)	-3.8543 (0.0001)	-3.2968 (0.0005)	-2.8036 (0.0025)	

**Table 7** The DM test results for different models in 3-month-ahead forecasting.

Countries	Models	B-SAKE	SAKE	B-KELM	KELM	B-MLP	MLP
US	SAKE	-1.9925 (0.0232)					
	B-KELM	-2.1426 (0.0161)	-1.9895 (0.0233)				
	KELM	-2.2567 (0.0120)	-2.1103 (0.0174)	-1.8803 (0.0300)			
	B-MLP	-2.8893 (0.0019)	-2.6177 (0.0044)	-1.9011 (0.0286)	-1.8511 (0.0321)		
	MLP	-3.6254 (0.0001)	-3.4526 (0.0003)	-2.0219 (0.0216)	-1.9416 (0.0261)	-1.7913 (0.0366)	
	SARIMA	-4.4029 (0.0000)	-4.2103 (0.0000)	-4.0014 (0.0000)	-3.8916 (0.0000)	-3.2341 (0.0006)	-2.6011 (0.0046)
UK	SAKE	-1.8365 (0.0331)					
	B-KELM	-1.9141 (0.0278)	-1.8854 (0.0297)				
	KELM	-2.1056 (0.0176)	-2.0112 (0.0222)	-1.8103 (0.0351)			
	B-MLP	-2.7319 (0.0031)	-2.5133 (0.0060)	-1.8995 (0.0287)	-1.8356 (0.0332)		
	MLP	-3.4103 (0.0003)	-3.2608 (0.0006)	-2.1236 (0.0169)	-2.0143 (0.0220)	-1.8041 (0.0356)	
	SARIMA	-4.3291 (0.0000)	-4.1890 (0.0000)	-4.0126 (0.0000)	-3.7859 (0.0001)	-3.2210 (0.0006)	-2.5961 (0.0047)
Germany	SAKE	-1.8511 (0.0321)					
	B-KELM	-1.9954 (0.0230)	-1.8453 (0.0325)				
	KELM	-2.1063 (0.0176)	-2.0043 (0.0225)	-1.8510 (0.0321)			

	B-MLP	-2.6917 (0.0036)	-2.3120 (0.0104)	-1.9013 (0.0286)	-1.8363 (0.0332)		
	MLP	-3.4011 (0.0003)	-3.3017 (0.0005)	-2.2163 (0.0133)	-2.1247 (0.0168)	-1.8142 (0.0348)	
	SARIMA	-4.2985 (0.0000)	-4.1066 (0.0000)	-3.9859 (0.0000)	-3.7956 (0.0001)	-3.3018 (0.0005)	-2.5385 (0.0056)
France	SAKE	-1.7995 (0.0360)					
	B-KELM	-1.8563 (0.0317)	-1.7956 (0.0363)				
	KELM	-1.9863 (0.0235)	-1.9983 (0.0228)	-1.8152 (0.0347)			
	B-MLP	-2.2106 (0.0135)	-2.1183 (0.0171)	-1.8025 (0.0357)	-1.8564 (0.0317)		
	MLP	-3.3142 (0.0005)	-3.1745 (0.0008)	-2.1195 (0.0170)	-2.0016 (0.0227)	-1.7974 (0.0361)	
	SARIMA	-4.1107 (0.0000)	-4.0135 (0.0000)	-3.8983 (0.0000)	-3.6968 (0.0001)	-3.1163 (0.0009)	-2.4101 (0.0080)

**Table 8** The DM test results for different models in 6-month-ahead forecasting.

Countries	Models	B-SAKE	SAKE	B-KELM	KELM	B-MLP	MLP
US	SAKE	-1.8013 (0.0358)					
	B-KELM	-2.0527 (0.0201)	-1.8416 (0.0328)				
	KELM	-2.2015 (0.0139)	-2.0234 (0.0215)	-1.7983 (0.0361)			
	B-MLP	-2.7749 (0.0028)	-2.4517 (0.0071)	-1.8546 (0.0318)	-1.7634 (0.0389)		
	MLP	-3.4135 (0.0003)	-3.2635 (0.0006)	-2.0034 (0.0226)	-1.8125 (0.0350)	-1.7011 (0.0445)	
	SARIMA	-4.2011 (0.0000)	-4.1063 (0.0000)	-3.9568 (0.0000)	-3.7412 (0.0001)	-3.0253 (0.0012)	-2.2103 (0.0135)
UK	SAKE	-1.7413 (0.0408)					
	B-KELM	-1.8041 (0.0356)	-1.7998 (0.0359)				
	KELM	-2.0143 (0.0220)	-1.9951 (0.0230)	-1.7654 (0.0387)			
	B-MLP	-2.5639 (0.0052)	-2.3674 (0.0090)	-1.8123 (0.0350)	-1.7741 (0.0380)		
	MLP	-3.3691 (0.0004)	-3.1231 (0.0009)	-2.1526 (0.0157)	-1.9526 (0.0254)	-1.6979 (0.0448)	
	SARIMA	-4.2141 (0.0000)	-4.0142 (0.0000)	-3.9896 (0.0000)	-3.6362 (0.0001)	-2.9958 (0.0014)	-2.2036 (0.0138)
Germany	SAKE	-1.7958 (0.0363)					
	B-KELM	-1.9011 (0.0286)	-1.7896 (0.0368)				
	KELM	-2.0034 (0.0226)	-1.9568 (0.0252)	-1.7963 (0.0362)			
	B-MLP	-2.4968 (0.0063)	-2.2691 (0.0116)	-1.8856 (0.0297)	-1.7985 (0.0360)		
	MLP	-3.2103 (0.0007)	-3.1029 (0.0010)	-2.0367 (0.0208)	-2.0014 (0.0227)	-1.7042 (0.0442)	
	SARIMA	-4.1953 (0.0000)	-4.0183 (0.0000)	-3.8561 (0.0001)	-3.6345 (0.0001)	-3.0152 (0.0013)	-2.3671 (0.0090)
France	SAKE	-1.7013 (0.0444)					
	B-KELM	-1.8354 (0.0332)	-1.7142 (0.0432)				
	KELM	-1.8964 (0.0290)	-1.9648 (0.0247)	-1.7969 (0.0362)			
	B-MLP	-2.1243 (0.0168)	-2.0356 (0.0209)	-1.9153 (0.0277)	-1.8015 (0.0358)		
	MLP	-3.1425 (0.0008)	-3.0142 (0.0013)	-2.0148 (0.0220)	-1.9686 (0.0245)	-1.7126 (0.0434)	
	SARIMA	-4.0968 (0.0000)	-3.9163 (0.0000)	-3.7853 (0.0001)	-3.5964 (0.0002)	-2.9354 (0.0017)	-2.2012 (0.0139)

**Table 9** The PT test results for different models.

Countries	Horizons	SARIMA	MLP	B-MLP	KELM	B-KELM	SAKE	B-SAKE
US	1-month-ahead	1.9856 (0.0471)	2.2013 (0.0277)	2.9856 (0.0028)	3.1025 (0.0019)	3.8842 (0.0001)	4.3568 (0.0000)	4.9158 (0.0000)
	3-month-ahead	1.8335 (0.0667)	2.0109 (0.0443)	2.7992 (0.0051)	2.8519 (0.0043)	3.6539 (0.0003)	4.0985 (0.0000)	4.5985 (0.0000)

UK	6-month-ahead	1.2096 (0.2264)	1.9803 (0.0477)	2.3981 (0.0165)	2.4913 (0.0127)	3.3981 (0.0007)	3.7251 (0.0002)	4.0856 (0.0000)
	1-month-ahead	1.9921 (0.0464)	2.2103 (0.0271)	2.9936 (0.0028)	3.1127 (0.0019)	3.8911 (0.0001)	4.3602 (0.0000)	4.9011 (0.0000)
	3-month-ahead	1.8435 (0.0653)	2.0127 (0.0441)	2.8024 (0.0051)	2.8893 (0.0039)	3.6694 (0.0002)	4.1025 (0.0000)	4.5894 (0.0000)
	6-month-ahead	1.2109 (0.2259)	1.9934 (0.0462)	2.3845 (0.0171)	2.5005 (0.0124)	3.4038 (0.0007)	3.7358 (0.0002)	4.0952 (0.0000)
Germany	1-month-ahead	1.9735 (0.0484)	2.1980 (0.0279)	2.8913 (0.0038)	3.0106 (0.0026)	3.7569 (0.0002)	4.2011 (0.0000)	4.7351 (0.0000)
	3-month-ahead	1.8037 (0.0713)	2.0014 (0.0453)	2.7971 (0.0052)	2.7985 (0.0051)	3.5050 (0.0005)	4.0023 (0.0001)	4.3958 (0.0000)
	6-month-ahead	1.2003 (0.2300)	1.9802 (0.0477)	2.2021 (0.0277)	2.4801 (0.0131)	3.3912 (0.0007)	3.6918 (0.0002)	3.9965 (0.0001)
France	1-month-ahead	1.9825 (0.0474)	2.1833 (0.0290)	2.7395 (0.0062)	3.0012 (0.0027)	3.6028 (0.0003)	4.2125 (0.0000)	4.6981 (0.0000)
	3-month-ahead	1.7953 (0.0726)	1.9952 (0.0460)	2.7102 (0.0067)	2.6528 (0.0080)	3.4167 (0.0006)	3.8996 (0.0001)	4.2896 (0.0000)
	6-month-ahead	1.1952 (0.2320)	1.9733 (0.0485)	2.1537 (0.0313)	2.3341 (0.0196)	3.2533 (0.0011)	3.5853 (0.0003)	3.9561 (0.0001)

## 4.5 Summary

In this section, we train the models and conduct numerical experiments adopting the following data related to travel demand, including historical data on tourist arrivals arriving in Beijing from four countries, economic indicators that affect tourism demand and online tourist behavior variables that reflect their concerns. The forecasting results of the proposed B-SAKE model and other benchmark models are compared. In summary, some interesting implications are obtained as follows:

(1) The proposed B-SAKE model achieves the highest forecasting accuracy via MAPE, NRMSE, and DS and outperforms the other benchmark models in the DM test and the PT test, followed by other AI models, whereas the SARIMA model ranks the last.

(2) Although the SARIMA model can effectively capture the periodicity caused by seasonal factors, it is not applicable to forecasting nonlinear, uncertain and irregular tourist data, in which nonlinear AI models have significant advantages.

(3) As an ensemble approach, bagging can effectively reduce the forecasting variance and improve the forecasting accuracy through the idea of the model average. Stacked autoencoders are used to a construct deep learning network to effectively solve the problem of feature learning.

(4) This study analyzes the forecasting power of the models based on tourist arrival data in Beijing from four countries and comes to a consistent conclusion, which illustrates the effectiveness and robustness of the method.

## 5. Conclusions and managerial implications

Due to the very large challenges in working with large amounts of data, a bagging-based multivariate ensemble deep learning model, integrating stacked autoencoders and KELM, is proposed for tourism demand forecasting. The data considered in this article include historical data on tourist arrivals in Beijing, economic indicators and online tourist behavior variables. The empirical study results indicate that our proposed B-SAKE model has forecasting accuracy and robustness. In particular, we analyze four

cases of forecasting tourist arrivals from four countries and reach consistent conclusions.

In the current era of big data, information and data are more accessible. Deep learning is good at discovering intricate relationships in data. Consequently, the proposed deep learning model can also be used to forecast other difficult problems, for instance, transport passenger flow forecasting, air transport demand forecasting and crude oil price forecasting. It is worth noting that weather, safety factors, and online comment data are not taken into consideration for the convenience of the calculations in this study. It is also meaningful to explore the preprocessing of these types of data and the construction of indicators related to tourism demand. In addition, automatically choosing appropriate parameters for the AI models remains an issue for further research.

The managerial implications of this study include the following three aspects: (1) The results of our forecasting can guide travel companies in the allocation of tourism resources, thus reducing unnecessary costs and creating excellent experiences for tourists. (2) Our proposed deep learning approach makes effective use of data, which provides guidelines for travel practitioners. (3) Our research provides the decision-making basis for government departments to formulate tourism policies and plan infrastructure construction.

### **Conflicts of interest**

The authors declare that they have no conflicts of interest regarding the publication of this study.

### **Authors' contributions list**

**Shaolong Sun** and **Ju-e Guo** conceived of the presented idea. **Shaolong Sun** developed the forecasting framework and performed the computations. **Shaolong Sun** contributed to the interpretation of the results. **Shouyang Wang** supervised the findings of this work. **Shaolong Sun** and **Yanzhao Li** participated in writing the manuscript. All the authors provided critical feedback and helped shape the research, analysis, and manuscript. All the authors read and approved the manuscript.

### **Acknowledgements**

This research work was partly supported by the National Natural Science Foundation of China under Grants No. 71988101 and No. 71642006.

## References

- Anderson, H. M., Athanasopoulos, G., & Vahid, F. (2007). Nonlinear autoregressive leading indicator models of output in G-7 countries. *Journal of Applied Econometrics*, 22(1), 63-87. doi:10.1002/jae.935
- Athanasopoulos, G., Hyndman, R. J., Song, H., & Wu, D. C. (2011). The tourism forecasting competition. *International Journal of Forecasting*, 27(3), 822-844. doi:https://doi.org/10.1016/j.ijforecast.2010.04.009
- Athanasopoulos, G., Song, H., & Sun, J. A. (2017). Bagging in tourism demand modeling and forecasting. *Journal of Travel Research*, 57(1), 52-68. doi:10.1177/0047287516682871
- Bangwayo-Skeete, P. F., & Skeete, R. W. (2015). Can Google data improve the forecasting performance of tourist arrivals? Mixed-data sampling approach. *Tourism Management*, 46, 454-464. doi:https://doi.org/10.1016/j.tourman.2014.07.014
- Bokelmann, B., & Lessmann, S. (2019). Spurious patterns in Google trends data - An analysis of the effects on tourism demand forecasting in Germany. *Tourism Management*, 75, 1-12. doi:https://doi.org/10.1016/j.tourman.2019.04.015
- Breiman, L. (1996). Bagging predictors. *Machine Learning*, 24(2), 123-140. doi:10.1007/BF00058655
- Bunn, D. (1989). Forecasting with more than one model. *Journal of Forecasting*, 8(3), 161-166. doi:10.1002/for.3980080302
- Carrière-Swallow, Y., & Labbé, F. (2013). Nowcasting with Google trends in an emerging market. *Journal of Forecasting*, 32(4), 289-298. doi:10.1002/for.1252
- Choi, H., & Varian, H. A. L. (2012). Predicting the present with Google trends. *Economic Record*, 88(s1), 2-9. doi:10.1111/j.1475-4932.2012.00809.x
- Chu, F.-L. (2011). A piecewise linear approach to modeling and forecasting demand for Macau tourism. *Tourism Management*, 32(6), 1414-1420. doi:https://doi.org/10.1016/j.tourman.2011.01.018
- Dergiades, T., Mavragani, E., & Pan, B. (2018). Google trends and tourists' arrivals: Emerging biases and proposed corrections. *Tourism Management*, 66, 108-120. doi:https://doi.org/10.1016/j.tourman.2017.10.014
- Diebold, F. X., & Mariano, R. S. (2002). Comparing predictive accuracy. *Journal of Business & Economic Statistics*, 20(1), 134-144. doi:10.1198/073500102753410444
- Fesenmaier, D. R., Xiang, Z., Pan, B., & Law, R. (2010). A framework of search engine use for travel planning. *Journal of Travel Research*, 50(6), 587-601. doi:10.1177/0047287510385466
- Ginsberg, J., Mohebbi, M. H., Patel, R. S., Brammer, L., Smolinski, M. S., & Brilliant, L. (2009). Detecting influenza epidemics using search engine query data. *Nature*, 457(7232), 1012-1014. doi:10.1038/nature07634
- Huang, G.-B. (2014). An insight into extreme learning machines: Random neurons, random features and kernels. *Cognitive Computation*, 6(3), 376-390. doi:10.1007/s12559-014-9255-2
- Huang, G.-B., Zhu, Q.-Y., & Siew, C.-K. (2006). Extreme learning machine: Theory and applications. *Neurocomputing*, 70(1), 489-501. doi:https://doi.org/10.1016/j.neucom.2005.12.126
- Inoue, A., & Kilian, L. (2008). How useful is bagging in forecasting economic time series? A case study of U.S. consumer price inflation. *Journal of the American Statistical Association*,



103(482), 511-522. doi:10.1198/016214507000000473

- Law, R., Li, G., Fong, D. K. C., & Han, X. (2019). Tourism demand forecasting: A deep learning approach. *Annals of Tourism Research*, 75, 410-423. doi:<https://doi.org/10.1016/j.annals.2019.01.014>
- Li, J., Xu, L., Tang, L., Wang, S., & Li, L. (2018). Big data in tourism research: A literature review. *Tourism Management*, 68, 301-323. doi:<https://doi.org/10.1016/j.tourman.2018.03.009>
- Li, S., Chen, T., Wang, L., & Ming, C. (2018). Effective tourist volume forecasting supported by PCA and improved BPNN using Baidu index. *Tourism Management*, 68, 116-126. doi:<https://doi.org/10.1016/j.tourman.2018.03.006>
- Li, X., Pan, B., Law, R., & Huang, X. (2017). Forecasting tourism demand with composite search index. *Tourism Management*, 59, 57-66. doi:<https://doi.org/10.1016/j.tourman.2016.07.005>
- Li, X., Wu, Q., Peng, G., & Lv, B. (2016). Tourism forecasting by search engine data with noise-processing. *African Journal of Business Management*, 10(6), 114-130. doi:10.5897/ajbm2015.7945
- Liu, Y., Chen, Y., Wu, S., Peng, G., & Lv, B. (2015). Composite leading search index: a preprocessing method of internet search data for stock trends prediction. *Annals of Operations Research*, 234(1), 77-94. doi:10.1007/s10479-014-1779-z
- Lv, S.-X., Peng, L., & Wang, L. (2018). Stacked autoencoder with echo-state regression for tourism demand forecasting using search query data. *Applied Soft Computing*, 73, 119-133. doi:<https://doi.org/10.1016/j.asoc.2018.08.024>
- Maqsood, H., Mehmood, I., Maqsood, M., Yasir, M., Afzal, S., Aadil, F., & Muhammad, K. (2020). A local and global event sentiment based efficient stock exchange forecasting using deep learning. *International Journal of Information Management*, 50, 432-451. doi:<https://doi.org/10.1016/j.ijinfomgt.2019.07.011>
- Pesaran, M. H., & Timmermann, A. (1992). A simple nonparametric test of predictive performance. *Journal of Business & Economic Statistics*, 10(4), 461-465. doi:10.1080/07350015.1992.10509922
- Pouyanfar, S., Sadiq, S., Yan, Y., Tian, H., Tao, Y., Reyes, M. P., & Iyengar, S. S. (2018). A survey on deep learning: Algorithms, techniques, and applications. *ACM Comput. Survey*, 51(5), 92
- Sagheer, A., & Kotb, M. (2019). Unsupervised pre-training of a deep LSTM-based stacked autoencoder for multivariate time series forecasting problems. *Scientific Reports*, 9(1), 19038. doi:10.1038/s41598-019-55320-6
- Shen, S., Li, G., & Song, H. (2008). An assessment of combining tourism demand forecasts over different time horizons. *Journal of Travel Research*, 47(2), 197-207. doi:10.1177/0047287508321199
- Song, H., Gao, B. Z., & Lin, V. S. (2013). Combining statistical and judgmental forecasts via a web-based tourism demand forecasting system. *International Journal of Forecasting*, 29(2), 295-310. doi:<https://doi.org/10.1016/j.ijforecast.2011.12.003>
- Song, H., & Li, G. (2008). Tourism demand modelling and forecasting-A review of recent research. *Tourism Management*, 29(2), 203-220. doi:<https://doi.org/10.1016/j.tourman.2007.07.016>
- Song, H., Qiu, R. T. R., & Park, J. (2019). A review of research on tourism demand forecasting: Launching the annals of tourism research curated collection on tourism demand forecasting. *Annals of Tourism Research*, 75, 338-362.

doi:<https://doi.org/10.1016/j.annals.2018.12.001>

- Stock, J. H., & Watson, M. W. (2012). Generalized shrinkage methods for forecasting using many predictors. *Journal of Business & Economic Statistics*, 30(4), 481-493. doi:10.1080/07350015.2012.715956
- Sun, S., Wei, Y., Tsui, K.-L., & Wang, S. (2019). Forecasting tourist arrivals with machine learning and internet search index. *Tourism Management*, 70, 1-10. doi:<https://doi.org/10.1016/j.tourman.2018.07.010>
- Yang, H.-F., & Chen, Y.-P. P. (2019). Representation learning with extreme learning machines and empirical mode decomposition for wind speed forecasting methods. *Artificial Intelligence*, 277, 103176. doi:<https://doi.org/10.1016/j.artint.2019.103176>
- Yang, X., Pan, B., Evans, J. A., & Lv, B. (2015). Forecasting Chinese tourist volume with search engine data. *Tourism Management*, 46, 386-397. doi:<https://doi.org/10.1016/j.tourman.2014.07.019>
- Yang, Y., Hong, W., & Li, S. (2019). Deep ensemble learning based probabilistic load forecasting in smart grids. *Energy*, 189, 116324. doi:<https://doi.org/10.1016/j.energy.2019.116324>
- Yin, H., Ou, Z., Huang, S., & Meng, A. (2019). A cascaded deep learning wind power prediction approach based on a two-layer of mode decomposition. *Energy*, 189, 116316. doi:<https://doi.org/10.1016/j.energy.2019.116316>
- Zhao, Y., Li, J., & Yu, L. (2017). A deep learning ensemble approach for crude oil price forecasting. *Energy Economics*, 66, 9-16. doi:<https://doi.org/10.1016/j.eneco.2017.05.023>